Supporting Information

SO_2-Tolerant NO_x Reduction by Marvellously Suppressing SO_2 Adsorption over $Fe_\delta Ce_{1-\delta}VO_4$ Catalysts

Lin Kang,† Lupeng Han,† Penglu Wang, Chong Feng, Jianping Zhang, Tingting Yan, Jiang Deng, Liyi Shi, and Dengsong Zhang*

International Joint Laboratory of Catalytic Chemistry, Department of Chemistry, State Key Laboratory of Advanced Special Steel, Research Center of Nano Science and Technology, College of Sciences, Shanghai University, Shanghai 200444, China

†These authors contributed equally to this work.

The Supporting Information includes 34 pages, 24 figures, and 2 tables.

Table of Contents

Characterization of Catalysts

The X-ray diffraction (XRD) experiments were carried out on a Rigaku D/MAS-RB X-ray diffractometer with Cu Kα (40 kV, 40 mA) radiation, and the XRD patterns were recorded in the 2θ range of 10° to 90° with a scan rate of 8 °/min. The microstructure of the catalyst was observed using a transmission electron microscope (TEM, JEM-200CX) and a high-resolution transmission electron microscope (HRTEM, JEM-2100F). The nitrogen adsorption-desorption isotherm of the samples were measured at -196 °C using an automatic surface and pore size analyzer (Autosorb-IQ2, Quantachrome Corporation), and the specific surface area of the sample was calculated by the Brunaue-Emmett-Teller (BET) method. The X-ray photoelectron spectroscopy (XPS) data of all the elements was obtained on a PerkinElmer PHI-5300CESCA system with Mg Kα radiation. The binding energies of Fe, Ce, V and O were calibrated for containment carbon (C 1s = 284.6 eV) as a reference. Visible Raman spectra were performed at room temperature on an inVia-reflex Renishaw spectrometer equipped with a holographic notch filter, a CCD detector and a 532 nm radiant laser.

The hydrogen temperature-programmed reduction (H_2-TPR), $O_2/NH_3/NO+O_2/SO_2+O_2$ temperature-programmed desorption ($O_2/NH_3/NO+O_2/SO_2+O_2$-TPD) was conducted on an auto-adsorption apparatus (TP-5080, Xianquan Industrial and Trading Co., Ltd) with the TCD detector (100 mA, 120 ºC, He as carrier gas) and an online mass spectrometer (OMNISTAR, Pfeiffer). Prior to the TPR or TPD process, the 80 mg sample was pretreated under a high purity Ar or He (99.999%) atmosphere with a flow rate of 30 mL/min for 30 min at 300 °C. For H_2-TPR, when the temperature cooled to room temperature, the gas was switched to 10% H_2/Ar, then the temperature was linearly raised to 800 °C at a rate of 10 °C/min. For $O_2/NH_3/NO+O_2/SO_2+O_2$-TPD, after cooling to 60 °C, the samples were exposed to a flow of 10%O_2/N_2, 10%NH_3/N_2, 500 ppm NO + 5%O_2/N_2 or 100 ppm SO_2

+ 5%O_2/N_2 for 1 h and then the gas was switched to He. Finally, the temperature was raised to 900 °C with heating rate of 10 °C/min. The breakthrough analysis of gas was carried out on a breakthrough analyzer (3P instrument mixSorb SHP). Before breakthrough analysis, 100 mg catalyst was pretreated under N_2 atmosphere with a flow rate of 30 mL/min for 30 min at 300 °C. When the temperature cooled to 240 ºC under nitrogen atmosphere, 0.4%NH_3/N_2, 0.4% NO/N_2, 0.4% SO_2/N_2, 0.4% SO_2/N_2 + 0.4% NO/N_2 or 0.4% SO_2/N_2 + 0.4% NH_3/N_2 was introduced to the catalyst to proceed the breakthrough analysis. For the NH_4HSO_4-TPDC experiment, 100 mg of catalysts pre-impregnated with 2 wt% NH_4HSO_4 were used. The temperature was raised to 900 °C with a ramping rate of 10 °C/min, and the off-gas was analyzed by MS. For the TPDC of sulfated catalysts, 100 mg of catalysts were used. The temperature was raised to 900 °C with a ramping rate of 10 °C/min, and the off-gas was analyzed by MS.

In situ diffuse reflectance infrared Fourier transform spectroscopy (*in situ* DRIFTs) experiments of samples were performed using a Nicolet 6700 spectrometer equipped with a Harrick Scientific DRIFT chamber and a MCT/A detector. The Kubelka–Munk collection range was from 1700 cm^{-1} to 1000 cm^{-1}, and the accumulating 64 scans with a resolution of 4 cm^{-1}. Prior to each test, the samples were pretreated at 300 °C for 30 min in a 50 mL/min N_2 gas stream. After pretreatment, the background spectrum of the sample was collected at the desired temperature, which was subtracted from the experimental results. In the adsorption and desorption behavior experiment, the sample was exposed to a flow of $NO + O_2$ (+ SO_2) or NH_3 at 30 °C for 1 h, then the desorption experiment was carried out under N_2 atmosphere and the results were recorded. In the case of transient reaction, the reaction temperature was fixed at 240 °C, the catalyst was exposed to $NO + O_2$ (+ SO_2) or NH_3 for 1 h, and then the gas was converted to NH_3 or $NO + O_2$ (+ SO_2), meanwhile recording the *in situ* DRIFTs

spectrum over time. The gas composition for *in situ* DRIFTs measurement conditions were 500 ppm NO, 500 ppm NH_3, 5 vol % O_2, 100 ppm SO_2 (when used), N_2 as the carrier gas.

Catalytic Performance Tests

The NH_3-SCR activity tests were performed using 0.3 g of catalysts (20-40 mesh) in a fixed-bed reactor with an inner diameter of 6 mm. The gas mixture composition were: [NO] = 500 ppm, [NH_3] = 500 ppm, [O_2] = 5 vol%, [H_2O] = 8 vol % (when used), [SO_2] = 100 ppm (when used), N_2 balance. The total flow rate was 250 mL/min, and the gas hourly space velocity (GHSV) was 60000 h^{-1}. The concentrations of NO_x, NH_3 and N_2O at the outlet of the reactor were measured by a 4000 VM analyzer, DR95C ammonia detector and G200 N_2O detector, respectively. The SCR catalytic activities were recorded after the reaction system reaches a steady state. The NO conversion rate is calculated by the following equation:

$$\text{NO conversion (\%)} = \frac{[NO]_{in}-[NO]_{out}}{[NO]_{in}} \times 100\ \%$$

$$N_2\ \text{selectivity (\%)} = \left(1-\frac{2[N_2O]_{out}}{[NO_x]_{in}+[NH_3]_{in}-[NO_x]_{out}-[NH_3]_{out}}\right) \times 100\ \%$$

Where NO_x stood for the total concentration of NO and NO_2. $[NO]_{in}$, $[NO]_{out}$, $[N_2O]_{out}$, $[NO_x]_{in}$, $[NO_x]_{out}$, $[NH_3]_{in}$, and $[NH_3]_{out}$ indicated the corresponding the inlet and outlet gas concentrations, respectively.

The GHSV was obtained by the following formula:

$$GHSV = \frac{q_v}{\pi hr^2}$$

q_v corresponded to the total flow rate; h meant the height of the catalyst in the reactor; and r represented the inner radius of the reactor.

All chemical reagents, provided by Sinopharm Chemical Reagent Co. Ltd (China), were of analytical grade and used without further purification.

Table S1. The textural properties of $CeVO_4$ and $Fe_\delta Ce_{1-\delta}VO_4$ catalysts.

Catalysts	Specific surface area ($m^2\ g^{-1}$)	Pore volume ($m^3\ g^{-1}$)	Average pore diameter (nm)
$CeVO_4$	43	0.26	3.43
$Fe_{0.1}Ce_{0.9}VO_4$	34	0.27	3.68
$Fe_{0.2}Ce_{0.8}VO_4$	33	0.27	3.58
$Fe_{0.3}Ce_{0.7}VO_4$	33	0.27	3.46
$Fe_{0.4}Ce_{0.6}VO_4$	33	0.26	3.59

Table S2. The amount of NH_3 desorption of $CeVO_4$ and $Fe_\delta Ce_{1-\delta}VO_4$ catalysts.

Catalyst	Weak acid sites (mmol/g)	Mediate acid sites (mmol/g)	Strong acid sites (mmol/g)	Total acid sites (mmol/g)
$CeVO_4$	1.27	—	3.91	5.18
$Fe_{0.1}Ce_{0.9}VO_4$	2.85	3.38	—	6.23
$Fe_{0.2}Ce_{0.8}VO_4$	3.08	3.63	—	6.71
$Fe_{0.3}Ce_{0.7}VO_4$	3.17	3.70	—	6.87
$Fe_{0.4}Ce_{0.6}VO_4$	3.13	3.17	—	6.30

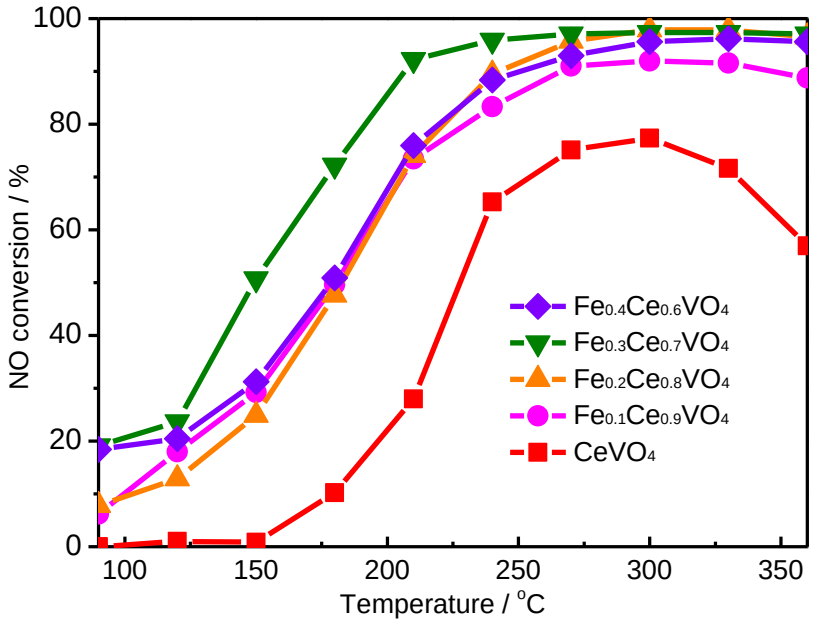

Figure S1. Plots of NO conversion and N_2 selectivity as a function of reaction temperature for $CeVO_4$ and $Fe_\delta Ce_{1-\delta}VO_4$ catalysts. Reaction conditions: 500 ppm NO, 500 ppm NH_3, 5 vol% O_2, N_2 as the balance gas, GHSV of 60000 h^{-1}.

Note: With increasing the content of Fe doping, the catalytic performance of $Fe_\delta Ce_{1-\delta}VO_4$ catalysts firstly improved for $Fe_{0.1}Ce_{0.9}VO_4$, $Fe_{0.2}Ce_{0.8}VO_4$ and $Fe_{0.3}Ce_{0.7}VO_4$ catalysts, and then declined for $Fe_{0.4}Ce_{0.6}VO_4$ catalyst.

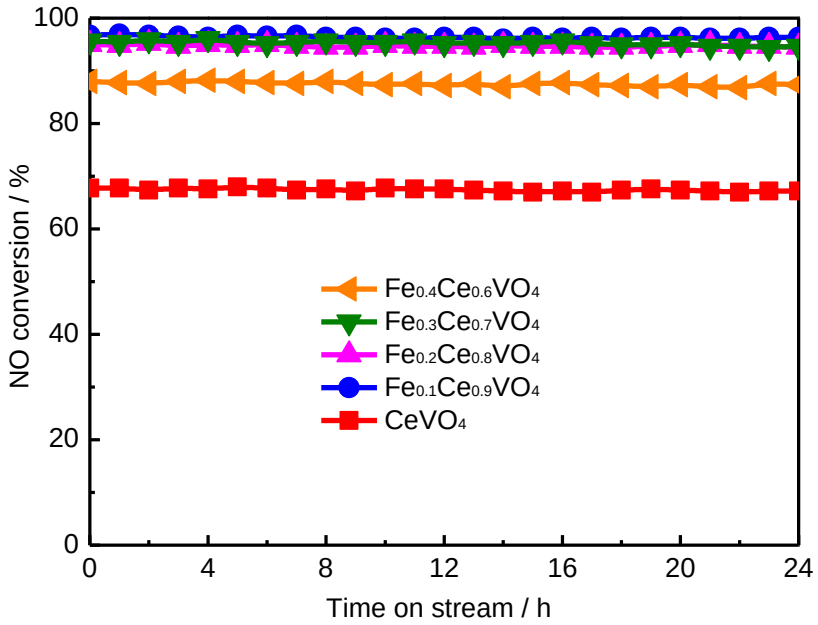

Figure S2. Stability tests of the $CeVO_4$ and $Fe_\delta Ce_{1-\delta}VO_4$ catalysts at 240 °C. Reaction conditions: 500 ppm NO, 500 ppm NH_3, 5 vol% O_2, N_2 as the balance gas, GHSV of 60000 h^{-1}.

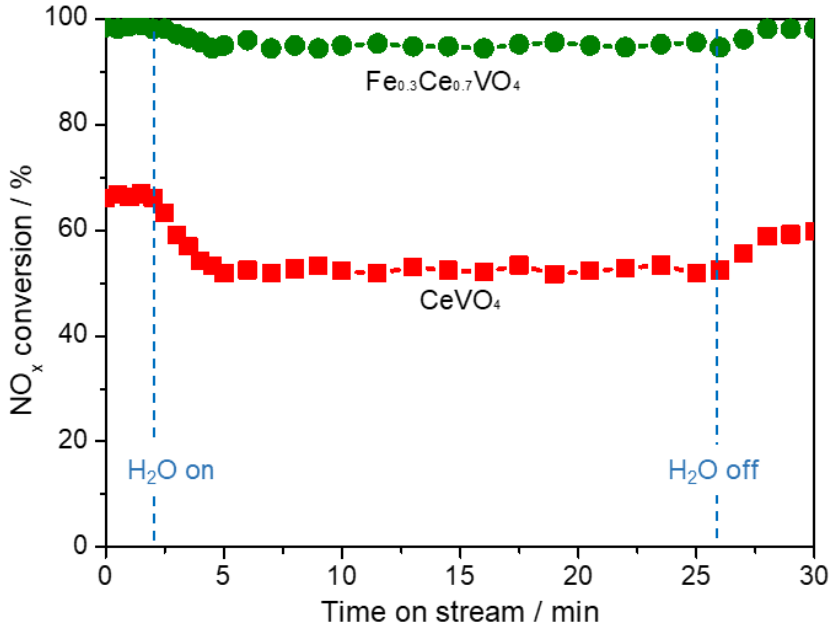

Figure S3. Plots of NO_x conversion *versus* time on stream over $CeVO_4$ and $Fe_{0.3}Ce_{0.7}VO_4$ catalysts in the presence of 8 vol% H_2O. Reaction conditions: 240 °C, 500 ppm NO, 500 ppm NH_3, 5 vol% O_2, N_2 as the balance gas, GHSV of 60000 h^{-1}.

Note: NO conversion of the $CeVO_4$ catalyst decreased from 66% to 52% and that of the $Fe_{0.3}Ce_{0.7}VO_4$ catalyst barely declined from 98% to 95%, revealing that of the water in the flue gas exhibited a relatively small effect on the de-NO_x activity of Fe doped $CeVO_4$ catalyst.

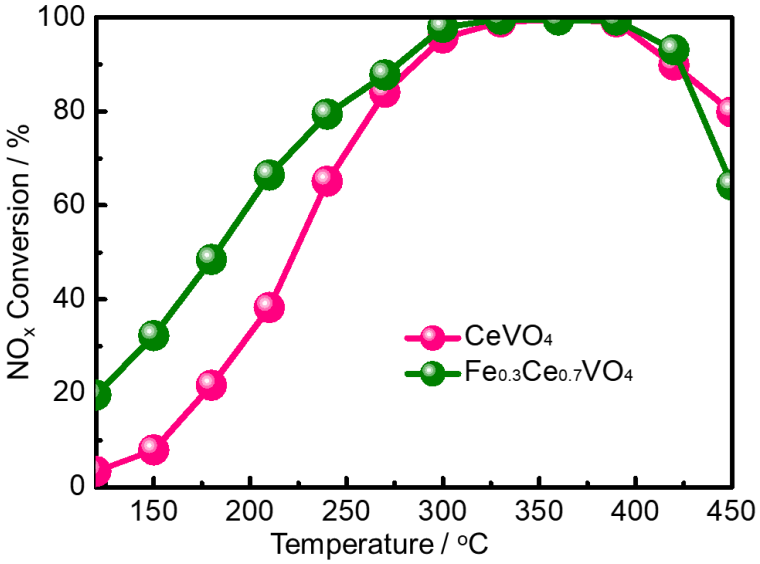

135

136 **Figure S4.** Plots of NO conversion as a function of reaction temperature for $CeVO_4$ and $Fe_{0.3}Ce_{0.7}VO_4$

137 catalysts in the presence of SO_2. Reaction conditions: 100 ppm SO_2, 500 ppm NO, 500 ppm NH_3, 5

138 vol% O_2, N_2 as the balance gas, GHSV of 60000 h^{-1}.

139

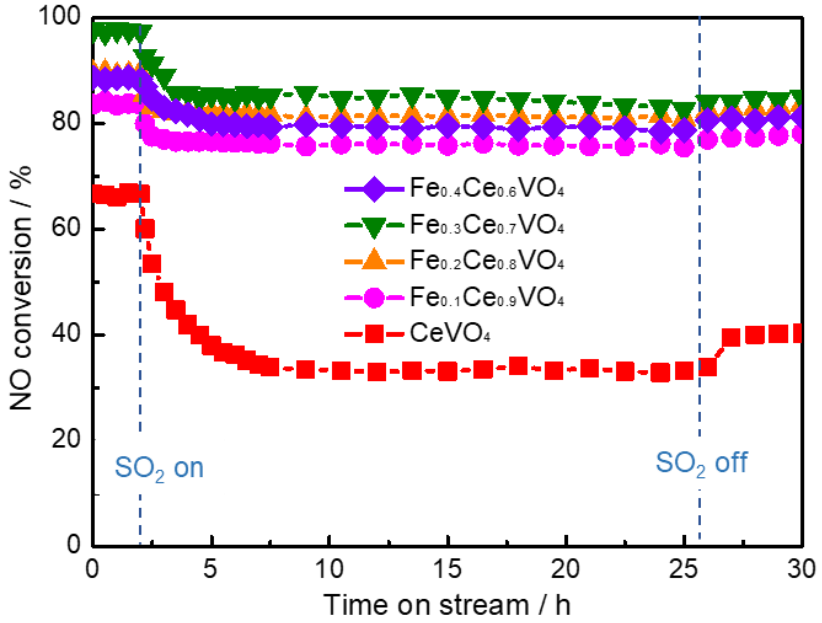

140

141 **Figure S5.** Plots of NO conversion *versus* time on stream over $CeVO_4$ and $Fe_\delta Ce_{1-\delta}VO_4$ catalysts in
142 the presence of SO_2 at 240 °C. Reaction conditions: 500 ppm NO, 500 ppm NH_3, 5 vol% O_2, 100
143 ppm SO_2, N_2 as the balance gas, GHSV of 60000 h^{-1}.

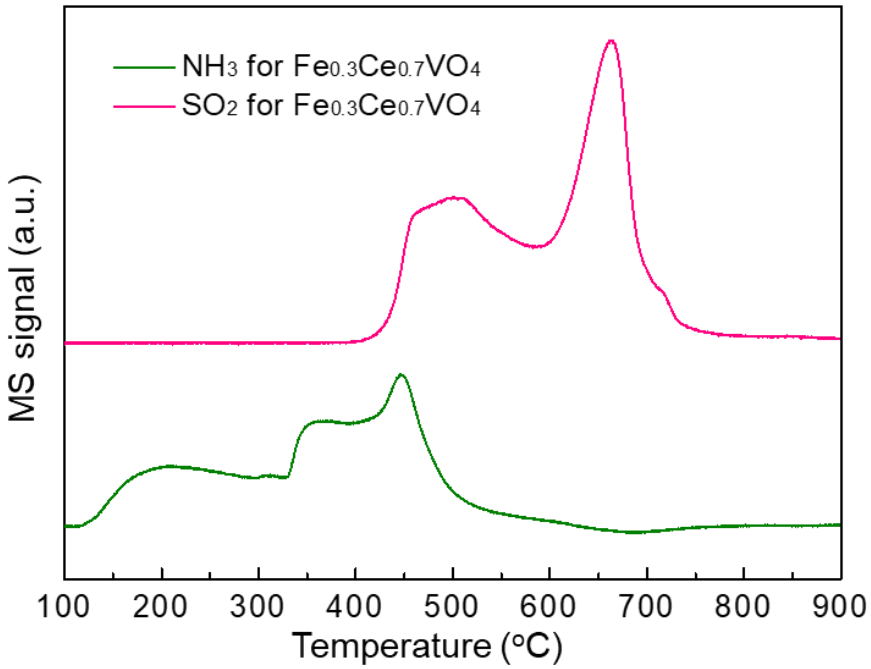

Figure S6. Temperature-programmed decomposition of $Fe_{0.3}Ce_{0.7}VO_4$ after reaction in the presence of SO_2 and H_2O for 10 h. Reaction conditions: 240 °C, 500 ppm of SO_2, 500 ppm of NO, 500 ppm of NH_3, 5 vol % O_2, N_2 as the balance gas, GHSV of 60000 h^{-1}.

Note: The NH_3 desorption between 300-500 ºC and the SO_2 desorption between 400-600 ºC could be attributed to the decomposition of NH_4HSO_4 while the SO_2 desorption above 600 ºC was related to the decomposition of cerium sulfate species.

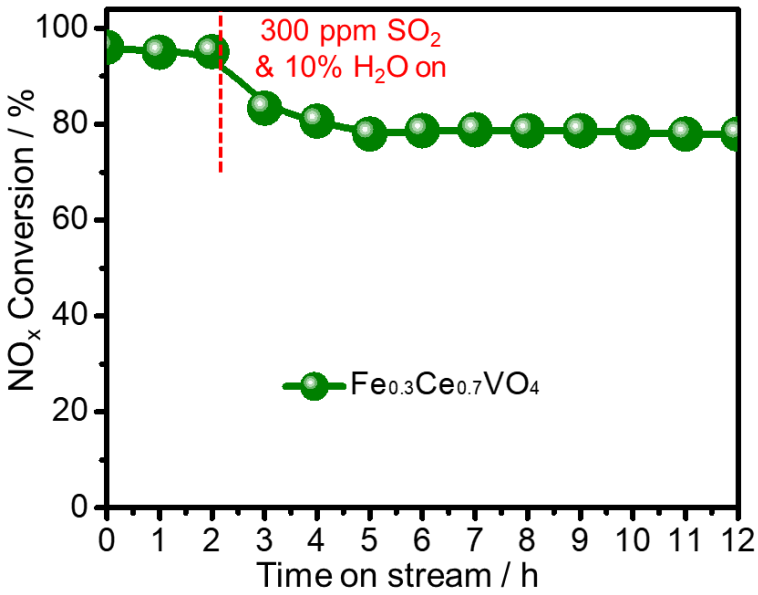

Figure S7. Plots of NO conversion *versus* time on stream over $Fe_{0.3}Ce_{0.7}VO_4$ catalysts in the presence of H_2O and SO_2 at 240 °C. Reaction conditions: 500 ppm NO, 500 ppm NH_3, 5 vol% O_2, 300 ppm SO_2, 10 vol% H_2O, N_2 as the balance gas, GHSV of 60000 h^{-1}.

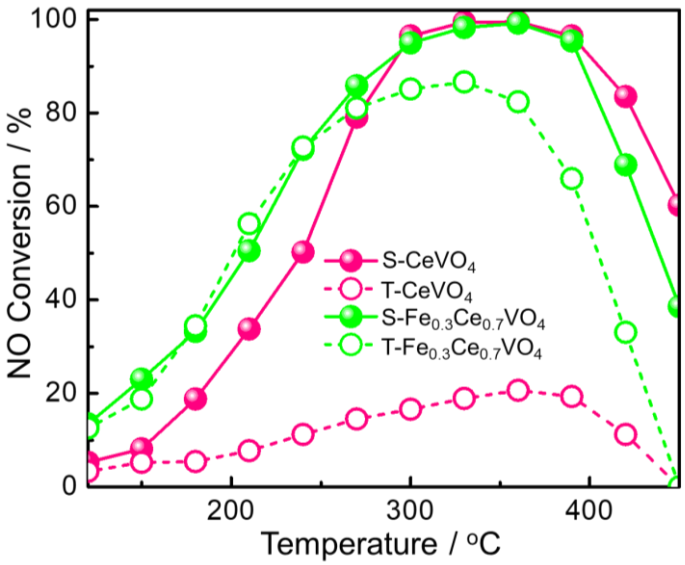

Figure S8. Plots of NO conversion *versus* temperature over sulfated and high-temperature treated $CeVO_4$ and $Fe_{0.3}Ce_{0.7}VO_4$. Sulfurization condition: 240 °C, GHSV of 60000 h^{-1}, 100 ppm SO_2, 5% O_2 in N_2, and sulfation time of 8 h. High-temperature treatment condition: 600 °C, 5% O_2 in N_2 GHSV of 60000 h^{-1}, and treatment of 2 h. S-$CeVO_4$ and S-$Fe_{0.3}Ce_{0.7}VO_4$ denoted sulfated $CeVO_4$ and $Fe_{0.3}Ce_{0.7}VO_4$, respectively; T-$CeVO_4$ and T-$Fe_{0.3}Ce_{0.7}VO_4$ denoted high-temperature treated $CeVO_4$ and $Fe_{0.3}Ce_{0.7}VO_4$, respectively.

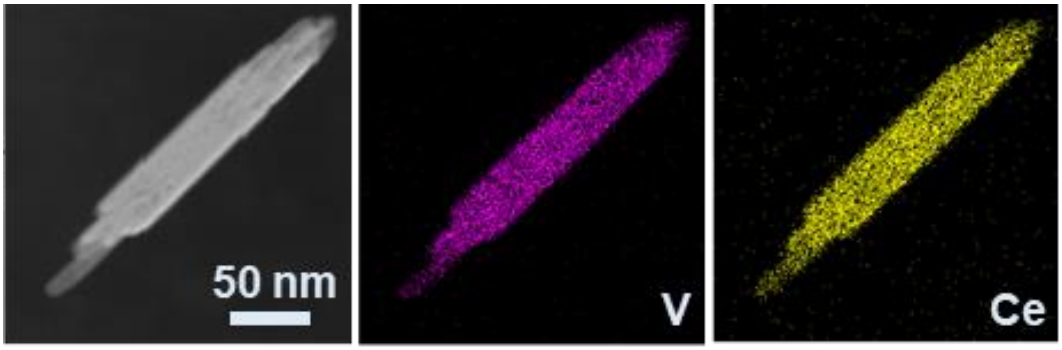

Figure S9. TEM-EDX mapping of the $CeVO_4$ catalyst.

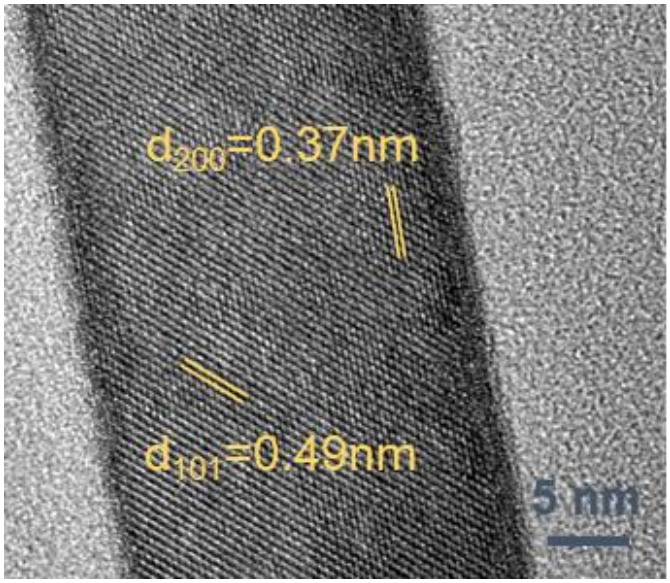

Figure S10. HRTEM image of the $CeVO_4$ catalyst.

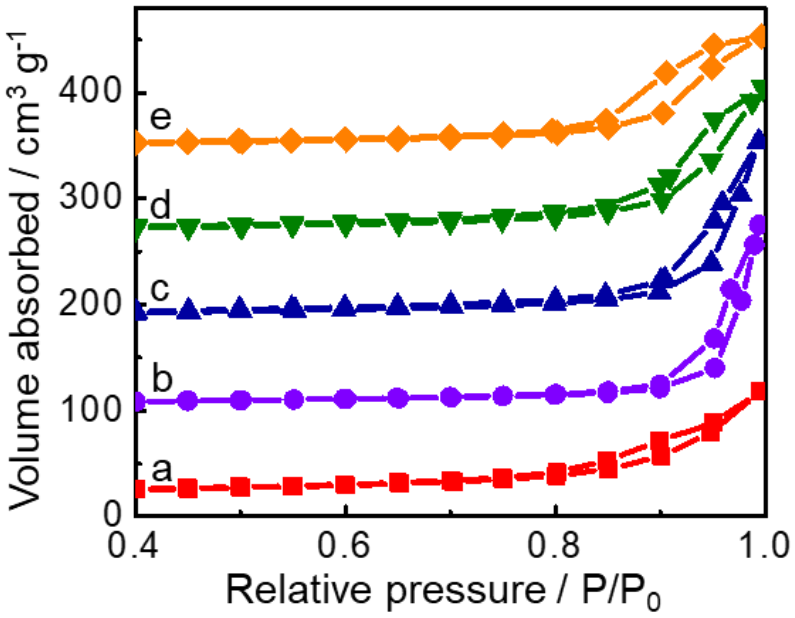

Figure S11. N_2 adsorption−desorption isotherm of $CeVO_4$ (a), $Fe_{0.1}Ce_{0.9}VO_4$ (b), $Fe_{0.2}Ce_{0.8}VO_4$ (c), $Fe_{0.3}Ce_{0.7}VO_4$ (d), and $Fe_{0.4}Ce_{0.6}VO_4$ (e) catalysts.

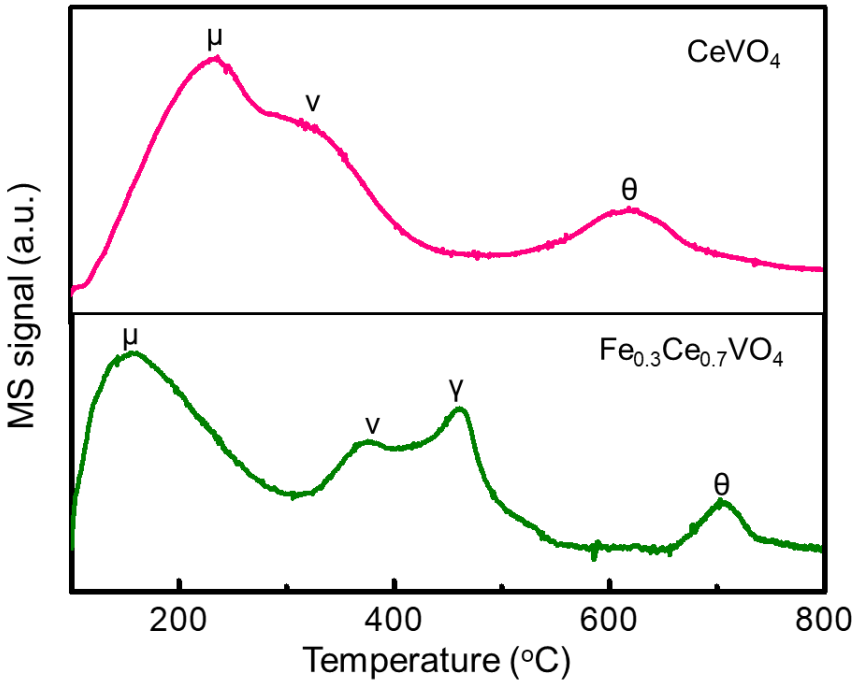

Figure S12. O_2-TPD profiles of $CeVO_4$ and $Fe_{0.3}Ce_{0.7}VO_4$ catalysts.

Note: For $CeVO_4$, the μ and ν peaks are related to the surface adsorbed oxygen species (O_α) while the θ peak is ascribed to the lattice oxygen species (O_β).[1] For $Fe_{0.3}Ce_{0.7}VO_4$, The μ, ν and γ peaks are related to the surface O_α species while the θ peak is ascribed to the O_β species. Via integrating the peak, the $O_\alpha/(O_\alpha + O_\beta)$ ratio is 87.5% for $CeVO_4$ and 94.9% for $Fe_{0.3}Ce_{0.7}VO_4$.

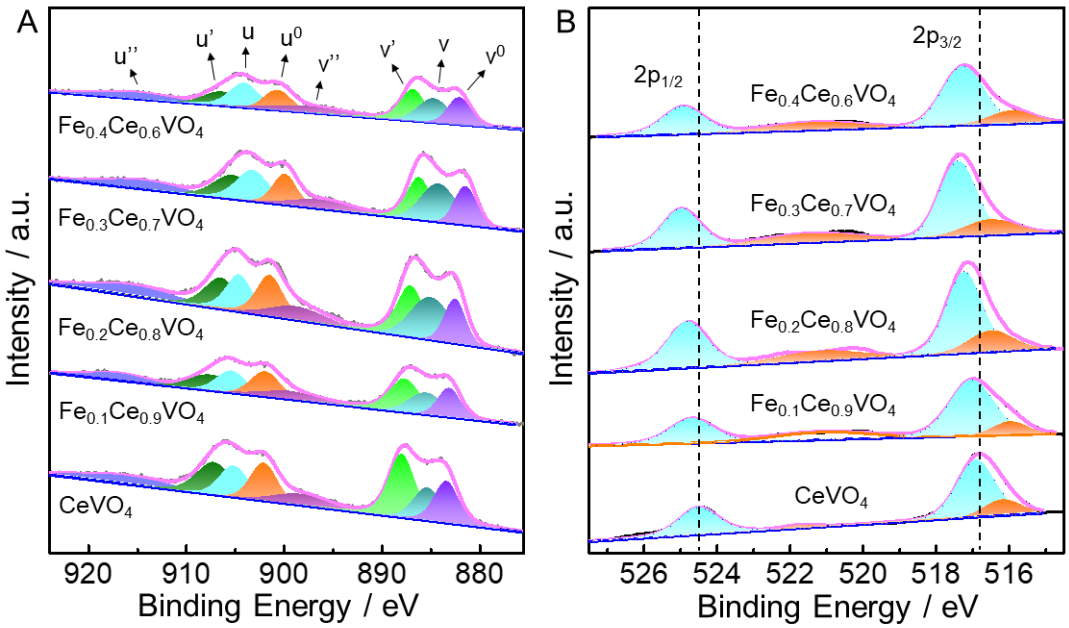

Figure S13. XPS spectra of (A) Ce 3d and (B) V 2p for $CeVO_4$ and $Fe_\delta Ce_{1-\delta}VO_4$ catalysts.

Note: The Ce 3d XPS results of all catalysts were divided into Ce $3d_{5/2}$ spin orbits ("v") and $3d_{3/2}$ spin orbits ("u"). The peaks labeled "u", "v" were the representatives of the $3d_{10}4f_1$ electronic state of the surface Ce^{3+} species, and the peaks assigned u^0, u', u", v^0, v', v" were corresponding to the $3d_{10}4f_0$ electronic state of Ce^{4+}.[2]

For the XPS spectra of V 2p, two characteristic binding energies mainly correspond to the two bonding states V $2p_{3/2}$ and V $2p_{1/2}$. In the $CeVO_4$ catalyst, the binding energy of V $2p_{3/2}$ was at 516.7 eV, and the binding energy of V $2p_{1/2}$ located at around 524.4 eV. Among them, the blue shaded portion was V^{5+} species, the orange curve represented V^{4+} species.[3]

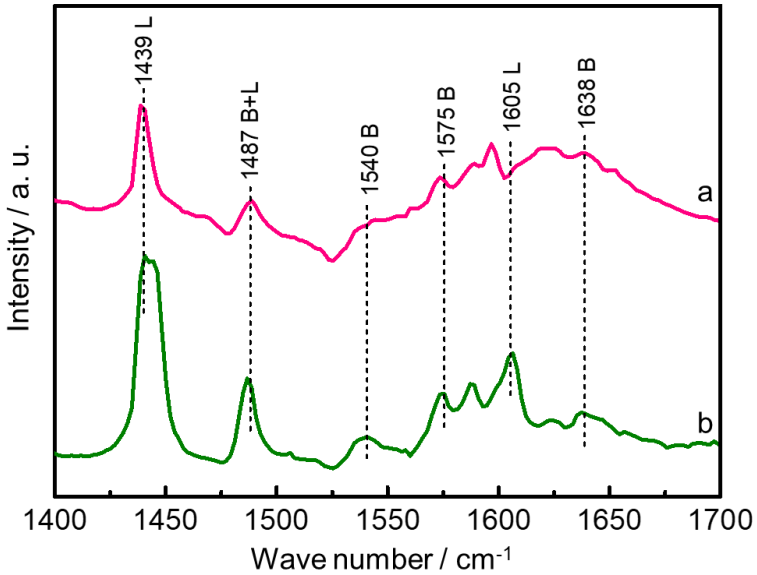

Figure S14. Pyridine-IR spectra at 150 °C over $CeVO_4$ (a) and $Fe_{0.3}Ce_{0.7}VO_4$ (b).

Note: The bands at 1439 and 1605 cm^{-1} were attributed to pyridine adsorbed onto Lewis acid, and those at 1540, 1575 and 1638 cm^{-1} were due to pyridine adsorbed onto Brønsted sites. The band at ~1487 cm^{-1} corresponded to the interaction of pyridine molecules with both Brønsted and Lewis acid sites.[4] It was found that there are more Brønsted and Lewis acid sites on $Fe_{0.3}Ce_{0.7}VO_4$ than those on $CeVO_4$.

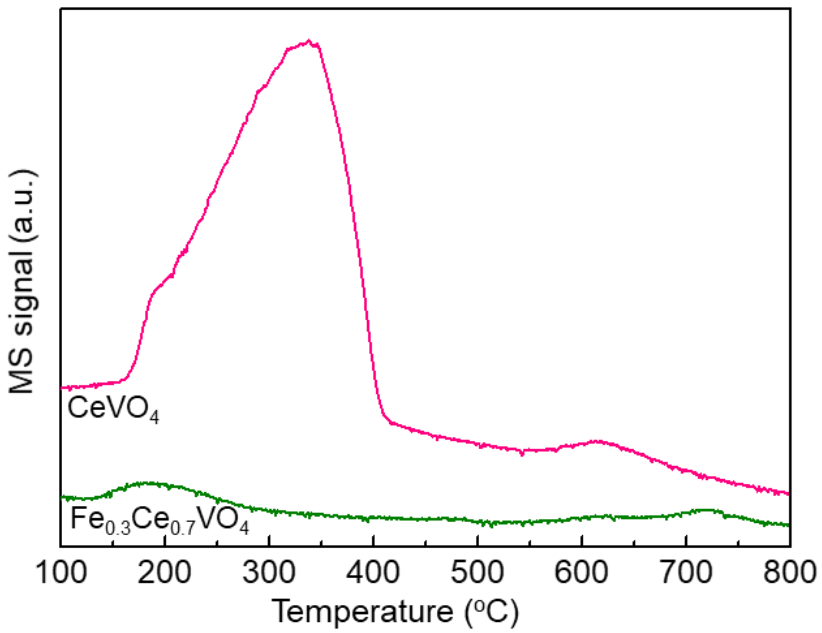

Figure S15. NO+O_2-TPD profiles of $CeVO_4$ and $Fe_{0.3}Ce_{0.7}VO_4$ catalysts.

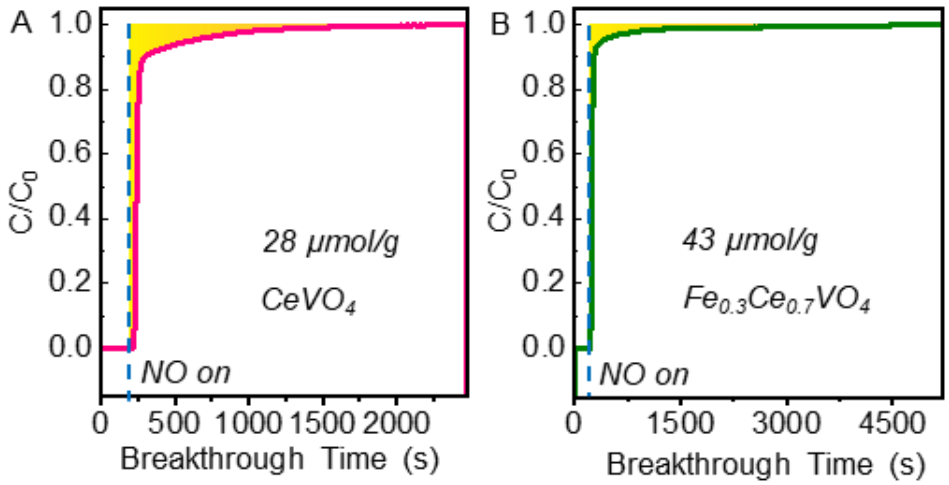

Figure S16. Profiles of *in situ* NO breakthrough over $CeVO_4$ (A) and $Fe_{0.3}Ce_{0.7}VO_4$ (B) at 240 °C.

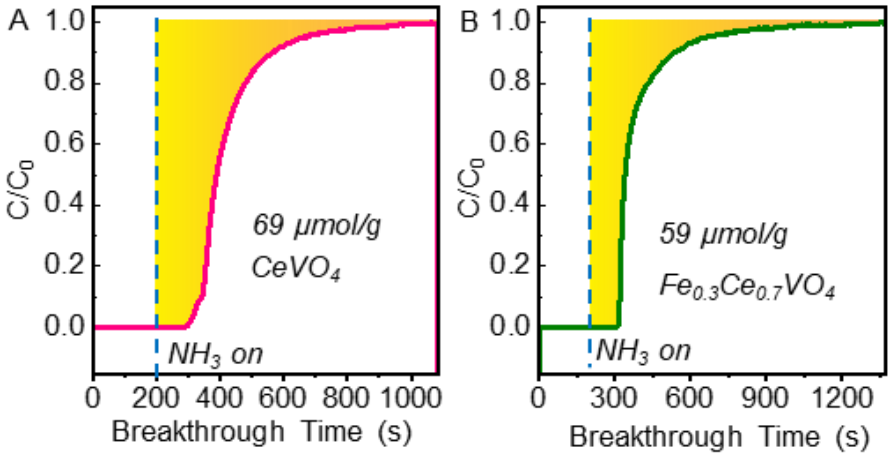

206

207 **Figure S17.** Profiles of *in situ* NH_3 breakthrough over $CeVO_4$ (A) and $Fe_{0.3}Ce_{0.7}VO_4$ (B) at 240 °C.

208

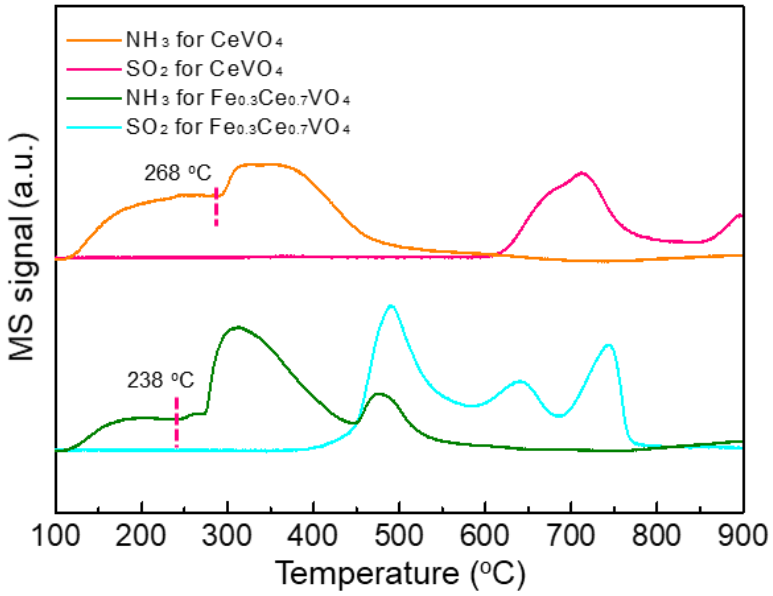

209

210 **Figure S18.** NH_4HSO_4-TPDC profiles of $CeVO_4$ and $Fe_{0.3}Ce_{0.7}VO_4$.

211

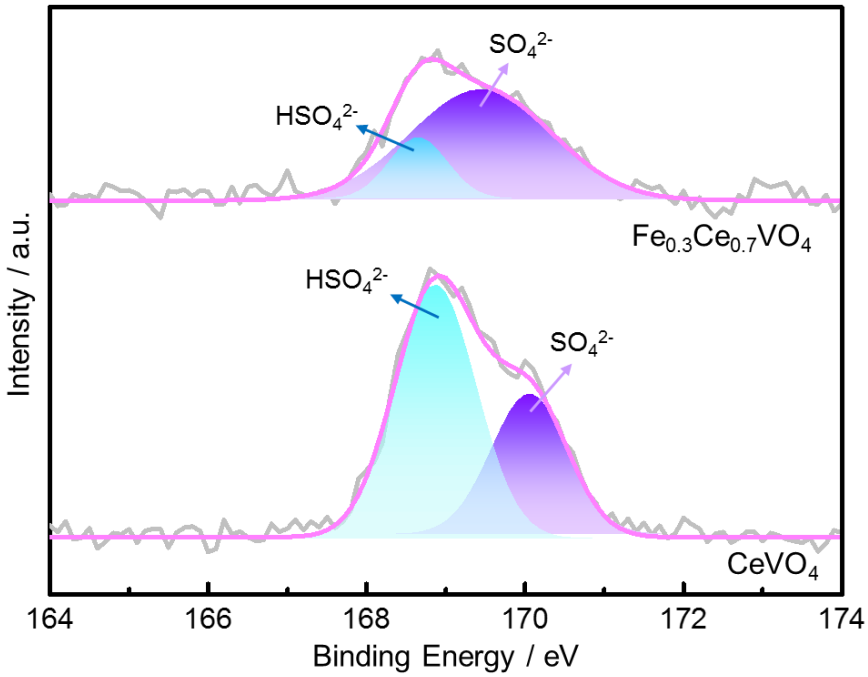

Figure S19. XPS spectra of S 2p for sulfated $CeVO_4$ and $Fe_{0.3}Ce_{0.7}VO_4$ catalysts.

Note: The sulfated catalysts were obtained by exposing the catalysts to a gas flow consisting of 500 ppm NO, 500 ppm NH_3, 5 vol% O_2 and 500 ppm SO_2 for 12 h at 240 °C. The S 2p peak with two binding energy at 169.5 and 168.7 eV, which could be assigned to SO_4^{2-} and HSO_4^{2-}, respectively.[5] It could be found that $Fe_{0.3}Ce_{0.7}VO_4$ had lower intensity of SO_4^{2-} and HSO_4^{2-} species, indicating fewer surface sulfates were formed.

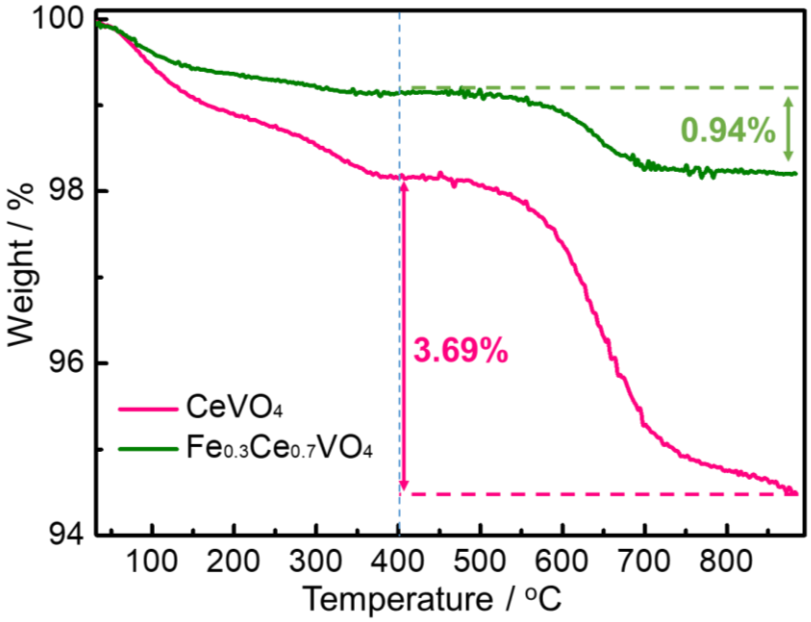

Figure S20. TGA curves of the catalysts after reaction in the presence of SO_2 and H_2O for 10 h. Reaction conditions: 240 °C, 300 ppm of SO_2, 10 vol% H_2O, 500 ppm of NO, 500 ppm of NH_3, 5 vol % O_2, N_2 as the balance gas, GHSV of 60000 h^{-1}.

Note: The weight loss below 400 °C was ascribed to the adsorbed water and the surface hydroxyl groups while the weight loss above 400 °C was attributed to the decomposition of NH_4HSO_4 and $CeSO_4$.[6] Above 400 °C, the weight loss of $CeVO_4$ was 3.69% and that of $Fe_{0.3}Ce_{0.7}VO_4$ was only 0.94%, indicating that much less sulfate species formed on $Fe_{0.3}Ce_{0.7}VO_4$ after reaction in the presence of H_2O and SO_2.

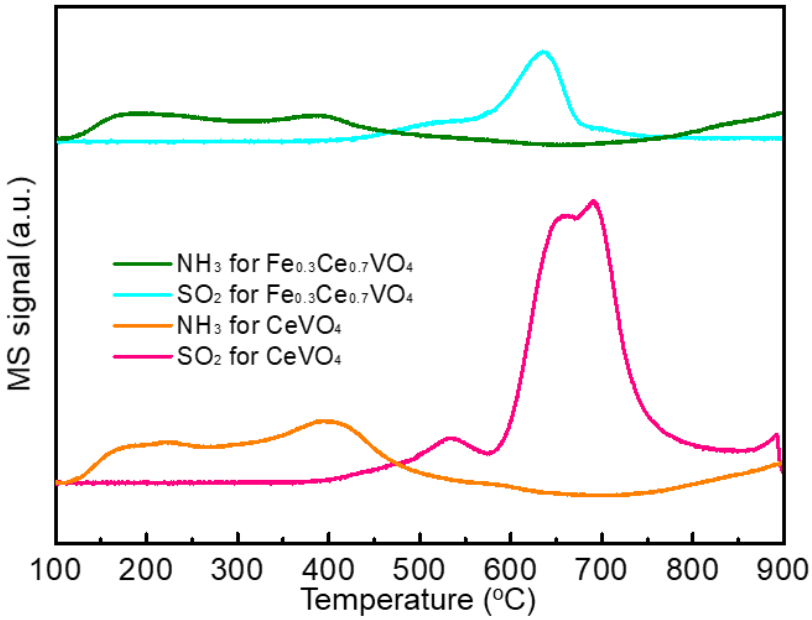

Figure S21. Temperature-programmed decomposition of catalysts after reaction in the presence of SO_2 and H_2O for 10 h. Reaction conditions: 240 °C, 300 ppm of SO_2, 10 vol% H_2O, 500 ppm of NO, 500 ppm of NH_3, 5 vol % O_2, N_2 as the balance gas, GHSV of 60000 h^{-1}.

Note: According to the intensity of SO_2 desorption, the amount of sulfate species deposited on $Fe_{0.3}Ce_{0.7}VO_4$ was much less than that on $CeSO_4$.

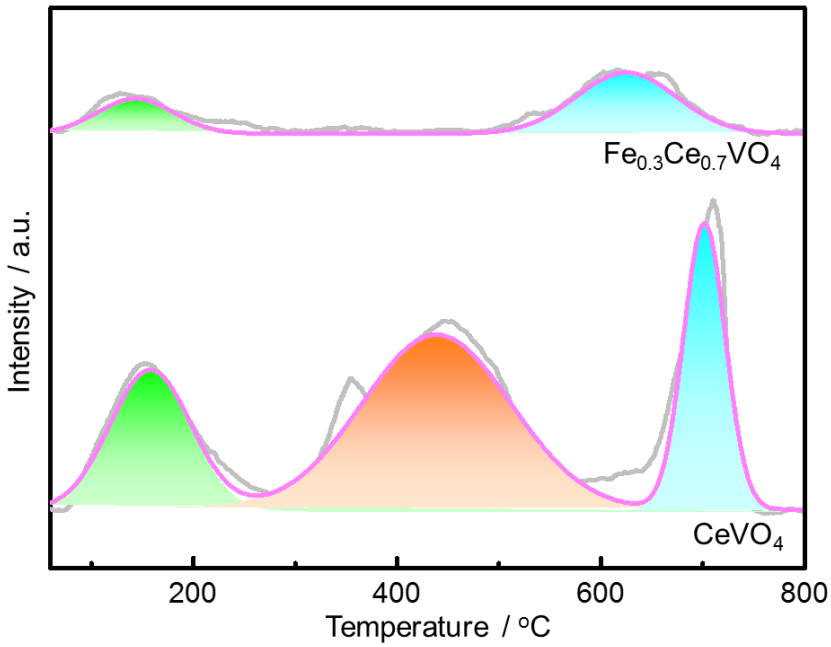

Figure S22. SO_2 + O_2-TPD profiles for $CeVO_4$ and $Fe_{0.3}Ce_{0.7}VO_4$ catalysts.

Note: Three types of sulfur species-related peaks could be observed in the $CeVO_4$ catalyst, namely the weakly adsorbed sulfur species desorbed from 100 °C to 300 °C,[7] the medium strength bonded sulfates desorbed from 300-550 °C, and the strongly bonded sulfate species desorbed above 550 °C.[8,9] However, the $Fe_{0.3}Ce_{0.7}VO_4$ catalyst showed only two desorption peaks belonging to weakly adsorbed SO_2 and strongly bonded sulfate species between 100 and 750 °C. The amount of weakly adsorbed SO_2 and strongly bonded sulfate species on the catalyst surface were largely reduced after the doping of Fe species. Therefore, it could be confirmed that the adsorption of SO_2 on the surface of the $Fe_{0.3}Ce_{0.7}VO_4$ catalyst was restrained after the addition of Fe, and the formation of sulfate was effectively inhibited.

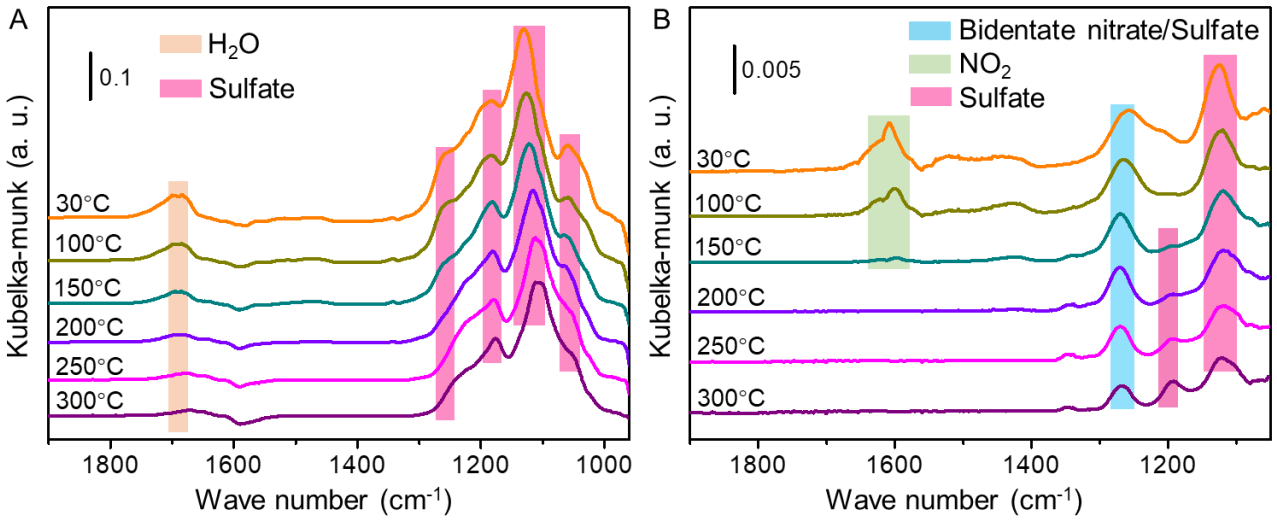

Figure S23. *In situ* DRIFTs of NO + O_2 + SO_2 desorption over $CeVO_4$ (A) and $Fe_{0.3}Ce_{0.7}VO_4$ (B) catalysts as a function of temperature.

Note: For $CeVO_4$, the band at 1689 cm^{-1} was attributed to the H_2O molecule. SO_2 can react with surface hydroxyl groups to generate H_2O and surface sulfite.[10] The bands at 1061, 1124, 1178 and 1258 cm^{-1} were attributed to the sulfate species.

For $Fe_{0.3}Ce_{0.7}VO_4$, the band at 1258 cm^{-1} were attributed to bidentate nitrate and sulfate species; the band at 1608 cm^{-1} was ascribed to the gaseous NO_2 species; the bands at 1124 and 1192 cm^{-1} were related to sulfate species.

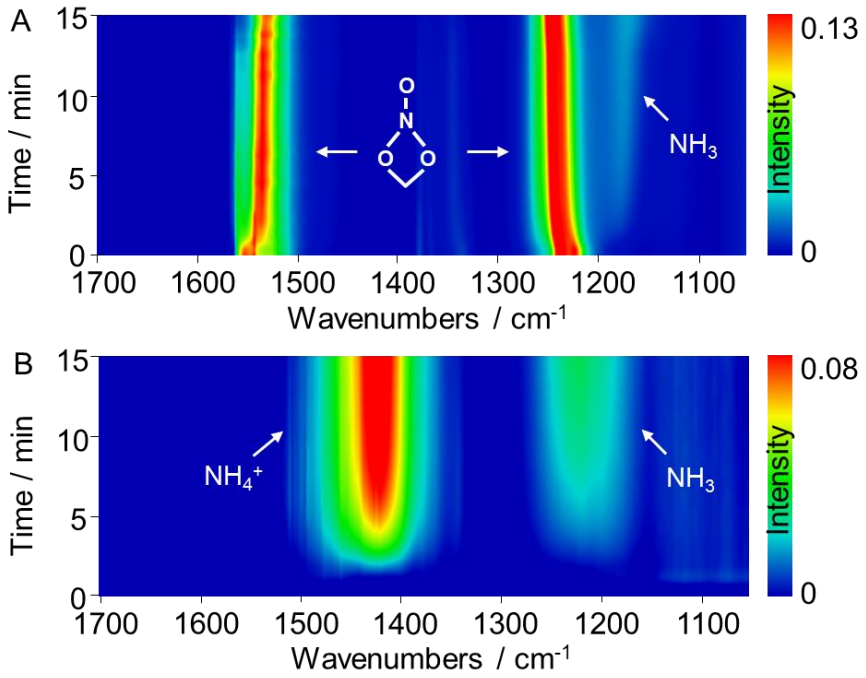

Figure S24. *In situ* DRIFTs of the (A) $CeVO_4$ and (B) $Fe_{0.3}Ce_{0.7}VO_4$ catalysts upon passing NH_3 over the catalysts with NO + O_2 pre-adsorbed at 240 °C as a function of time.

REFERENCES

(1) Li, P.; He, C.; Cheng, J.; Ma, C. Y.; Dou, B. J.; Hao, Z. P. Catalytic oxidation of toluene over Pd/Co_3AlO catalysts derived from hydrotalcite-like compounds: Effects of preparation methods. *Appl. Catal., B* **2011**, *101*, 570-579.

(2) Xu, H.; Liu, S.; Wang, Y.; Lin, Q.; Lin, C.; Lan, L.; Wang, Q.; Chen Y. Promotional effect of Al_2O_3 on WO_3/CeO_2-ZrO_2 monolithic catalyst for selective catalytic reduction of nitrogen oxides with ammonia after hydrothermal aging treatment. *Appl. Surf. Sci.* **2018**, *427*, 656-669.

(3) Wang, L.; Zhao, J.; Bai, S.; Zhao, H.; Zhu, Z. Significant catalytic effects induced by the electronic interactions between carboxyl and hydroxyl group modified carbon nanotube supports and vanadium species for NO reduction with NH_3 at low temperature. *Chem. Eng. J.* **2014**, *254*, 399-409.

(4) Sun, P.; Wang, W.; Weng, X.; Dai, X.; Wu, Z. Alkali potassium induced HCl/CO_2 selectivity enhancement and chlorination reaction inhibition for catalytic oxidation of chloroaromatics. *Environ. Sci. Technol*. **2018**, *52*, 6438-6447.

(5) Yu, Y.; Miao, J.; Wang, J.; He, C.; Chen, J. Facile synthesis of $CuSO_4/TiO_2$ catalysts with superior activity and SO_2 tolerance for NH_3-SCR: physicochemical properties and reaction mechanism. *Catal. Sci. Technol.*, **2017**, *7*, 1590-1601.

(6) Han, L.; Gao, M.; Feng, C.; Shi, L.; Zhang, D. Fe_2O_3-CeO_2@Al_2O_3 Nanoarrays on Al-Mesh as SO_2-Tolerant Monolith Catalysts for NO_x Reduction by NH_3. *Environ. Sci. Technol*. **2019**, *53*, 5946-5956.

(7) Yan, Q.; Chen, S.; Zhang, C.; Wang, Q.; Louis, B. Synthesis and catalytic performance of $Cu_1Mn_{0.5}Ti_{0.5}O_x$ mixed oxide as low temperature NH_3-SCR catalyst with enhanced SO_2 resistance. *Appl. Catal., B* **2018**, *238*, 236-247.

(8) Wang, H.; Qu, Z.; Dong, S.; Tang, C. Mechanistic investigation into the effect of sulfuration on the FeW catalysts for the selective catalytic reduction of NO_x with NH_3. *ACS Appl. Mater. Interfaces*

2017, *9*, 7017-7028.

(9) Yan, Q.; Nie, Y.; Yang, R.; Cui, Y.; O'Hare, D.; Wang, Q. Highly dispersed Cu_yAlO_x mixed oxides as superior low-temperature alkali metal and SO_2 resistant NH_3-SCR catalysts. *Appl. Catal., A* **2017**, *538*, 37-50.

(10) Gao, S.; Wang, P.; Yu, F.; Wang, H.; Wu, Z. Dual resistance to alkali metals and SO_2: vanadium and cerium supported on sulfated zirconia as an efficient catalyst for NH_3-SCR. *Catal. Sci. Technol.*, **2016**, *6*, 8148-8156.